JBC Papers in Press. Published on April 25, 2003 as Manuscript M300784200

A comparative functional analysis of plasma membrane Ca^{2+} pump isoforms in intact cells

Marisa Brini*, Luisa Coletto, Nicola Pierobon, Natasha Kraev#,

Danilo Guerini• and Ernesto Carafoli

Department of Biochemistry and Center for the Study of Biomembranes of the National Research Council (CNR), University of Padova, Viale G. Colombo 3, 35121 Padova; Venetian Institute of Molecular Medicine (VIMM), Via G. Orus 2, 35129 Padova, Italy and

•Transplantation Research Laboratory, Novartis Pharma AG, 4056 Basle, Switzerland.

*Corresponding author

e-mail: marisa.brini@unipd.it

phone: +39.049.8276167

fax: +39.049.8276125

[#]Present address: Department of Anaesthesia, University of Toronto, 200 Elizabeth Street, EN11-423, Toronto ON, Canada.

Running title

In vivo function of PMCA isoforms

The four basic isoforms of the plasma membrane Ca^{2+} pump and the two C-terminally truncated spliced variants PMCA4CII (4a) and 3CII (3a) were transiently overexpressed in Chinese hamster ovary cells together with aequorin targeted to the cytosol, the endoplasmic reticulum and the mitochondria. As PMCA3CII (3a) had not yet been cloned and studied, it was cloned for the study, partially purified, and characterized. At variance with the corresponding truncated variant of PMCA4, which had been studied previously PMCA3CII (3a) had very high calmodulin affinity. All four basic pump variants influenced the homeostasis of Ca^{2+} in the native intracellular environment. The level of Ca^{2+} refilling in the endoplasmic reticulum and the height of the [Ca^{2+}] transients generated in the cytosol and in the mitochondria by the emptying of the endoplasmic reticulum store by inositol 1,4,5-trisphosphate were all reduced by the overexpression of the pumps. The effects were much greater with the neuron-specific PMCA2 and PMCA3 than with the ubiquitously expressed isoforms 1 and 4. Unexpectedly, the truncated PMCA3 and PMCA4 were as effective as the full length variants in influencing the homeostasis of Ca^{2+} in the cytosol and the organelles. In particular, PMCA4CII (4a) was as effective as PMCA4CI (4b), even if its affinity for calmodulin is much lower. The results indicate that the availability of calmodulin may not be critical for the modulation of PMCA pumps *in vivo*.

Introduction

The plasma membrane calcium pumps (PMCAs) belong to the family of P-type ATPases, which are characterised by the formation of an aspartyl phosphate intermediate during the reaction cycle (1). Four genes encode distinct isoforms in mammals. PMCA1 and 4 are ubiquitously expressed, whereas PMCA2 and PMCA3 are predominantly expressed in the central nervous system (2). Alternative RNA splicing, occurring mostly at two sites termed A and C, generate additional isoform variability. C-site splicing occurs in the C-terminal region containing the calmodulin-binding domain. In the resting state, the latter interacts with two sites in the PMCA molecule, maintaining it inhibited (3, 4). Calmodulin removes the binding domain from these intramolecular receptors, freeing the pump from autoinhibition.

C site splicing occurs in the isoforms 1 and 3 through the piecemeal inclusion of portions of a 154 bp exon within the calmodulin-binding domain. The equivalent human variants of PMCA2 and 4 result instead from the inclusion of 227 bp and 178 bp exons, respectively (5). When the entire 154, 227, 178 bp exons are inserted the reading frame is lost, leading to the truncation of the pump at a stop codon located about 50 residues upstream of the C-terminus. The resulting proteins (termed CII, or a variant, according to the two prevailing nomenclatures used for PMCA isoforms) lack about half of the calmodulin-binding domain and thus differ significantly from the full-length variants termed CI (or b). In muscle and

neuronal cells the expression of basic and spliced PMCA isoforms is developmentally regulated. Tissue-specific factors are also likely to control the splicing of primary transcripts, since spliced isoforms have specific tissue distribution.

PMCAs have high Ca^{2+} affinity and thus maintain the basal sub-μM level of intracellular calcium (6, 7). The functional properties**,** the biochemical regulation, and the sequences and role of functional domains of the PMCA pump are now reasonably well clarified . One aspect which is not understood is the rationale for the multiplicity of isoforms and for their tissue specific expression. It would be logical to imagine that the isoforms differ in functional properties to accommodate the diverse Ca^{2+} homeostasis demands of various cell types. Unfortunately, information on functional differences among isoforms is very scarce.

Three PMCAs (PMCA1, 2, and 4) have been expressed in eukaryotic cells and some of their functional properties have been established. Significantly, the sensitivity to calmodulin is 3-4 times higher in PMCA2 than in the other isoforms (8). Some information is also available on the functional properties of spliced isoforms, i.e., the C-terminally truncated variant PMCA4CII (4a) has decreased affinity for calmodulin (9). The CII (a) variant of PMCA3 was expressly cloned in this study, to compare it to PMCA4CII (4a): unexpectedly, its calmodulin affinity is as high as that of full-length variants. Studies using the expressed recombinant C-terminal portion of the pump containing the calmodulin-binding domain have shown that splicing at site C confers pH sensitivity to the binding of calmodulin (10). A C-terminally spliced variant of PMCA3, termed 3f (or 3CVI), in which a short insert leads to the loss of most of the C-terminal portion downstream of the calmodulin-binding domain (11) has also been analysed. This isoform, which has been detected in skeletal muscle and to a lesser extent in brain, has very weak calmodulin affinity (12, 13). Unfortunately, these studies were

performed on isolated pump domains or on membrane preparations from overexpressing mammalian or insect cells in which possible physiological pump regulators may have become lost.

It was thus decided to study the activity of PMCA isoforms under physiological conditions by transfecting CHO[1] cells with expression plasmids for the four basic isoforms and for the two truncated variants 4CII (4a) and 3CII (3a) together with the plasmids encoding the Ca^{2+}-sensing probe aequorin targeted to the cytoplasm, to the mitochondria and to the endoplasmic reticulum (ER). At variance with fluorescent dyes, aequorin has very low Ca^{2+} buffering capacity, and does not significantly perturb the resting cytosolic Ca^{2+} level, which could influence the activity of the Ca^{2+} transporters.

The work has shown that the isoforms typical of neurons were more effective in restoring the basal [Ca^{2+}] level after the transient induced by an inositol 1,4,5-trisphosphate ($InsP_3$) generating agonist than the ubiquitously expressed isoforms. The two neuronal isoforms reduced [Ca^{2+}] in the ER by about 30%, whereas PMCA4 only decreased it by about 15%. Isoform 1 was even less effective, reducing ER [Ca^{2+}] only marginally. The effects on mitochondrial Ca^{2+} uptake, which reflect the level of Ca^{2+} filling of the ER (14), went along the same lines, i.e., the ubiquitous isoforms reduced it much less than PMCA2 and PMCA3. Unexpectedly, under the conditions of the CHO cell environment, essentially no differences in the effects on cytosolic, ER and mitochondrial [Ca^{2+}] were observed between the full-

[1]The abbreviation used are: CHO, Chinese hamster ovary cells; ER, endoplasmic reticulum; $InsP_3$, inositol 1,4,5-trisphosphate; PAGE, polyacrylamide gel; PMSF, phenylmethylsulfonyl fluoride; DTT, dithiothreitol; BCIP, 5-bromo-4-chloro-3-indolyl-phosphate; NBT, nitroblue tetrazolium; BSA, bovine serum albumin; PBS, phosphate-buffered saline; FITC, fluorescein isothiocyanate; erAEQ, ER-targeted aequorin; cytAEQ, cytosolic-targeted aequorin; mtAEQ, mitochondrially targeted aequorin; KRB, Krebs-Ringer buffer.

length pumps and the two truncated versions of PMCA3 and PMCA4.

Experimental procedures

Oligonucleotides were obtained from MWG Biotech (Münchenstein, Germany), and Microsinth AG (Balgach, Switzerland). The following primers have been used:

hPMCA3-1	5’	AGA TCG ACG AGA GCT CCC TGA C
hPMCA3-2	5’	TGC GGA GCT CCC GCT CGG CAT
hPMCA3-5	5’	GGC ACC ATA TGC ATC GCC TAC CGC GAC
hPMCA3-6	5’	GTA GGC GAT GCA TAT GGT GCG GAG GCC
hPMCA3-7	5’	CGA TGC ATA TGG TGC GGA GGC CAT C

The restriction sites are underlined.

Preparation of the construct for the hPMCA3CII (3a) isoform

The cDNA for the human PMCA3CII (3a) was assembled from fragments of the same. A short overview of the strategy used is outlined in Figure 1. Two partial clones containing the 5’ end (800 bp) and the 3’ end (1,000 bp) of the isoform were obtained by screening human brain libraries. The missing portion encompassing the central portion of the hPMCA3 cDNA was obtained by RT-PCR using human brain tissue and oligonucleotides hPMCA3-1/hPMCA3-5 and hPMCA3-2/hPMCA3-5. The two fragments obtained (A, 1,200 bp and B, 1,300 bp) were ligated via the NsiI site that was inserted with the help of hPMCA3-5 and hPMCA3-6 oligonucleotides. A SacI-BamHI 800 bp fragment encompassing the 5’ end of the PMCA3 cDNA was obtained from a partial cDNA clone and was ligated via the SacI site present in the A fragment in the pUC BM20 vector (Roche-Boeringer, Rotkreuz, Switzerland). To obtain the full-length cDNA a 500 bp ApaI-ApaI cDNA fragment containing the 3’ region of the hPMCA3CII (3a) isoform was inserted in the pUC BM20

3,300 bp construct. The clones with the correct orientations were selected by DNA sequencing. The full-length final construct was sequenced in both directions and found to be identical to that published by (15) with the exception of the NsiI site at position 2061.

The full-length cDNA (3,880 bp) in pTZ18/R was digested with KpnI-SalI and cloned in the corresponding sites of the pFastBac vector (Life Technologies, Inc., Basle, Switzerland) to generate recombinant baculoviruses carrying the complete coding sequence of the hPMCA3CII (3a) isoform.

Cell cultures and transfections

Spodoptera frugiperda (Sf9) cells were grown in TNM-FH supplemented with 10% fetal calf serum and 100 µg/ml gentamicin at 29 ± 1°C. All routine procedures involving these cells were performed according to (16). The recombinant baculoviruses were prepared according to the manufacturer's protocol (Invitrogen Ltd, Paisley, UK), (17). The transfer vectors needed to produce recombinant viruses were prepared by cloning the chimeric constructs (generated in pSG5) in BamHI-KpnI sites of pFastBac (Invitrogen). Transfection with a supercoiled DNA purified using a Maxi Kit (QIAGEN, Basle, Switzerland) was performed using SuperFect (QIAGEN) according to the supplier's protocol.

For the experiments on the co-expression of the pumps with aequorin, CHO cells were grown in Ham's F12 medium, supplemented with 10% fetal calf serum, in 75 cm^2 Falcon flasks. Before transfection, they were seeded onto 13 mm glass coverslips or on 24-multiwell plates (for Western blotting analysis) and allowed to grow to 50% confluence. At this stage, transfection with 3 µg of plasmid DNA (or 1.5:1.5 µg in the case of co-transfection) was carried out as previously described (18). The plasmids were all from the human variants of

the pump with the exception of that for PMCA3CI (kindly donated by Dr. E. E. Strehler, Rochester, MN) that was from rat. The amino acidic sequence homology of rat and human PMCA3 exceeds 99%. Aequorin measurements, immunocytochemistry and Western blotting analysis were performed 36 h later.

Preparation of membranes from Sf9 cells

Sf9 cells were collected two days after infection with recombinant baculoviruses, washed three times in 25 mM Tris-HCl, pH 7.5, 150 mM NaCl, and homogenized in 10 mM Tris-HCl, pH 7.5 (40 strokes of a Dounce homogenizer, on ice), in the presence of 75 µg/ml phenylmethylsulfonyl fluoride (PMSF), 100 U/ml Trasylol and 1 mM dithiothreitol (DTT). After the addition of sucrose and KCl to a final concentration of 10% and 150 mM, respectively, the nuclei and gross debris were sedimented for 10 min at 750 x *g* 10 mM EDTA was added to the post-nuclear supernatant, which was sedimented at 100,000 x *g* for 45 min. The high-speed pellet was resuspended in 4 mM Tris-HCl, pH 7.5 and 10% sucrose and stored at -70^{o}C.

SDS-PAGE and Western blotting of Sf9 cells membranes

Proteins were separated on sodium dodecylsulfate polyacrylamide gels (SDS-PAGE) essentially according to (19). Samples were boiled 5 min after the addition of one volume of 0.5 M DTT, 5% SDS, 6 M urea, 50 mM Tris-HCl, pH 8.0 and 1.5 mM EDTA.

Polyacrylamide gel electrophoresis under acidic conditions to detect the phosphorylated intermediate was performed according to (20). The samples were dissolved at room temperature in 65 mM Tris-phosphate, pH 6.8, 0.5 M DTT, 5% SDS, 6 M urea, 5 mM

EDTA. The electrophoresis buffer contained 170 mM MOPS, adjusted to pH 6.0 with Tris-base, and 0.1% SDS.

The proteins separated by SDS-PAGE were transferred to nitrocellulose sheets (21), which were blocked overnight at room temperature in 2% gelatin (Fluka, Buchs, Switzerland) in TBS (10 mM Tris-HCl, pH 8.0, 150 mM NaCl). The primary antibodies were applied for 1-2 h at room temperature. The polyclonal antibody 3N, raised in rabbits against the N-terminal domain of hPMCA3, (2, 22) was used at a 1/500 dilution in TBST (10 mM Tris-HCl, pH 8.0, 150 mM NaCl, 0.05% Tween-20 and 1 mM $CaCl_2$). The monoclonal antibody 5F10 (Affinity Bioreagent, Inc., Golden, Co) which recognises all PMCA isoforms (23) was used at a 1/3,000 dilution. After washing, the blots were incubated for 1 h at room temperature with alkaline phosphatase-coupled secondary antibodies (Promega, Madison, WI USA) diluted 1/7000 in TBST. The blots were developed with the colour substrates 5-bromo-4-chloro-3-indolyl-phosphate (BCIP) and nitroblue tetrazolium (NBT) (ProtoBlot system, Promega).

Calmodulin overlay

Proteins were transferred to nitrocellulose sheets (21). Nonspecific binding of calmodulin was blocked by 1% bovine serum albumin (BSA) in TBST. The blots were incubated separately with different concentrations of biotinylated calmodulin (1 nM to 1 μM in TBST) for 1 h, washed twice in TBST and incubated for another hour with avidin-coupled alkaline phosphatase in TBST. The filters were developed with 66 μl NBT and 33 μl BCIP (Promega) in 10 ml alkaline phosphatase buffer (100 mM Tris-HCl, pH 9.0, 100 mM NaCl, 5 mM $MgCl_2$ and 1 mM $CaCl_2$).

Formation of the phosphoenzyme intermediate

The formation of the phosphoenzyme intermediate from ATP was studied on membranes obtained from Sf9 cells infected with recombinant viruses. 25-50 µg of membrane proteins were resuspended in 50 µl of 20 mM MOPS-KOH, pH 6.8, 100 mM KCl, in the presence of 100 µM $CaCl_2$ and 100 µM $LaCl_3$. The reaction, carried out on ice, was started by the addition of 0.3 µM γ-^{32}P-ATP (300 Ci/mmoles) and stopped 30 sec later by adding 6% trichloroacetic acid/1 mM Pi. The samples were kept on ice for 15 min and then spun down at 15,000 x *g* for 20 min at 4°C. The pellets were washed with 6% trichloroacetic acid/1 mM Pi and with distilled water. They were resuspended in sample buffer, separated on acidic SDS-PAGE (20), dried, and analysed by autoradiography. When using partially purified proteins, Ca^{2+} and La^{3+} were added to an approximate final concentration 1 mM each. The presence of EDTA, Mg^{2+} and other components in the media used for the purification procedure prevented the precise calculation of the free concentrations of the two cations. In some cases, after phosphorylation the trichloroacetic acid-precipitated pellet was resuspended in 0.2 M NH_2OH for 30 min at room temperature, and precipitated again by 6% trichloroacetic acid /1 mM Pi, prior to applying it to the gel.

Purification of the overexpressed pumps

Membranes of infected Sf9 cells were prepared as described above. All purification steps were carried out at 4°C. The solubilisation of the membrane proteins was performed by addition of Triton X-100 to a final concentration of 0.4% and to a detergent to protein weight ratio of about 1/1. Crude membranes were incubated for 20 min on a rotatory table and centrifuged at 100,000 x g for 30 min using a Beckman CTL-100 ultracentrifuge. Egg yolk L-α-phosphatidylcholine was added to the collected supernatant to a final concentration of

0.5 mg/ml, glycerol to a final concentration of 15% (v/v), DTT to a final concentration of 3 mM and $CaCl_2$ to a final concentration of up to 50 μM.

The solubilised proteins were incubated for at least 2 h or overnight with calmodulin-Sepharose 4B in an equilibration buffer containing 20 mM HEPES, pH 7.2, 130 mM NaCl, 1 mM $MgCl_2$, 100 μM $CaCl_2$, 0.4 % Triton X-100, 0.5 mg /ml egg yolk L-α-phosphatidylcholine, 15% glycerol (v/v) and 3 mM DTT. The calmodulin-Sepharose 4B was sedimented by centrifugation. The resin was repeatedly washed and sedimented using at least 10 volumes of equilibration buffer, and then with at least 10 volumes of equilibration buffer with reduced Triton X-100 concentration (0.05%). It was then packed into a column from which the ATPase was finally eluted with a buffer containing 20 mM HEPES, pH 7.2, 130 mM NaCl, 1 mM $MgCl_2$, 2 mM EDTA, 0.05 % Triton X-100, 0.5 mg /ml egg yolk L-α-phosphatidylcholine, 15% glycerol (v/v) and 3 mM DTT. The buffer was sonicated before use. The collected fractions were pooled, divided into small aliquots and stored at -70°C. They were analysed on 7 or 10 % SDS-PAGE which were stained by a silver nitrate procedure.

Calmodulin-Sepharose 4B

Recombinant calmodulin was immobilised on CNBr-activated-Sepharose 4B according to the procedure supplied by the manufacturer (Amersham-Pharmacia, Buckinghamshire, UK). The yield of the coupling reaction was controlled by SDS-PAGE.

Measurement of Ca^{2+}-ATPase activity

The Ca^{2+}-ATPase activity was measured by the colorimetric method described by (24). The

reaction buffer contained 20 mM HEPES, pH 7.2, 100 mM KCl and 0.5 mM EGTA. $CaCl_2$ was added to the final free concentrations indicated in the individual experiments. They were calculated with the computer program described by (25). The reaction was performed in a final volume of 100 µl in the presence of 1 mM ATP. The incubation times were 30 min or 2 h, at 37 °C.

Immunolocalization of the expressed pumps

Thirty-six hours after transfection, CHO cells were processed for immunofluorescence as follows: they were washed twice with phosphate-buffered saline (PBS; 140 mM NaCl, 2 mM KCl, 1.5 mM KH_2PO_4, 8 mM Na_2HPO_4 pH 7.4), fixed for 20 min in 3.7% formaldehyde, washed three times with PBS and then incubated for 10 min in PBS supplemented with 50 mM NH_4Cl. They were permeabilised in 0.1% Triton X-100 in PBS, followed by a 1 h wash with 1% gelatin (type IV, from calf skin) in PBS. Cells were then incubated for 1 h at 37°C in a wet chamber with antibody 5F10, at a 1:100 dilution in PBS. Staining was then carried out with fluorescein isothiocyanate (FITC)-labelled anti-mouse secondary antibodies (Dako, Glostrup, Denmark) at a 1:50 dilution in PBS. After each incubation, cells were washed four times with PBS. Fluorescence was then analysed with a Bio-Rad 2100MP confocal system (Bio-Rad, Hercules, CA). FITC-conjugated antibody was excited with a 488nm Ar Laser and emission filtered through a 485/30 bandpass filter.

Preparation of membranes from CHO cells and Western blotting analysis

Thirty-six hours after transfection, CHO cells were harvested in 10 mM Tris-HCl, pH 8.0, 2

mM EDTA, 2 mM PMSF, 1 mM DTT. They were disrupted by three cycles of freeze and thaw at –80°C/37°C and the insoluble proteins were sedimented at 11,000 x *g* for 30 min (4°C). The supernatant was discarded and the pellet resuspended in 5 mM Tris-HCl, pH 8.0, and 10% sucrose. Proteins were separated by 7.5% SDS-PAGE and transferred to nitrocellulose membranes. 100 µg of membrane proteins were loaded onto each lane. The sheets were probed with antibody 5F10 (diluted 1:1,000). After incubation with anti-mouse horseradish peroxidase-conjugated secondary antibodies (Santa Cruz Biotechnology, Santa Cruz, CA) the blots were developed with ECL reagents (Amersham Bioscience Europe GmbH, Milan, Italy). The quantitative analysis was carried out by densitometric analysis using the Kodak 1D Image Analysis program (Kodak Scientific Imaging System, New Haven, CT).

Aequorin measurements

The Ca^{2+} content of the ER had to be drastically reduced before the reconstitution of functional erAEQ. To this end cells were incubated for 1 h at 4°C in KRB (125 mM NaCl, 5 mM KCl, 1 mM Na_3PO_4, 1 mM $MgSO_4$, 5.5 mM glucose, 20 mM HEPES pH 7.4, 37°C) supplemented with 5 µM coelenterazine n and the Ca^{2+} ionophore ionomycin (5 µM) and 600 µM EGTA. After this incubation, the cells were washed extensively with KRB supplemented with 2% BSA and 1 mM EGTA and transferred to the chamber of a custom-built luminometer.

Transfected cytAEQ and mtAEQ were reconstituted by incubating the cells for 1–3 h with 5 µM wild type coelenterazine in Dulbecco's modified Eagle's medium supplemented with 1%

FCS, at 37°C in a 5% CO_2 atmosphere.

The additions to the KRB medium (1 mM $CaCl_2$, 100 μM ATP) were made as specified in the Figures. The experiments were terminated by lysing the cells with 100 μM digitonin in a hypotonic Ca^{2+}-rich solution (10 mM $CaCl_2$ in H_2O) to discharge the remaining aequorin pool. The light signal was collected and calibrated into $[Ca^{2+}]$ values as previously described (18, 26, 27, 28). In brief, a 13 mm round coverslip with the transfected cells was placed in a perfused thermostated chamber placed in close proximity to a low-noise photomultiplier, with a built-in amplifier discriminator. The output of the discriminator was captured by a Thorn-EMI photon counting board and stored in an IBM-compatible computer for further analyses. The aequorin luminescence data were calibrated off-line into $[Ca^{2+}]$ values, using a computer algorithm based on the Ca^{2+} response curve of wild type and mutant aequorins, as previously described (26, 27).

Results

Cloning, partial purification and characterisation of PMCA3CII (3a)

To construct a full-length expression vector for PMCA3CII (3a), nucleotide mutations were inserted in the coding sequence, generating a NsiI site at position 2061 (Figure 1). These modifications did not result in amino acid changes. Even if several PCR-based steps were performed, the final construct did not contain unexpected mutations, as verified by sequencing the final construct in both directions. The truncated PMCA3 was

expressed using the baculovirus system in parallel with the PMCA4CI (4b) variant, which had been already expressed in previous studies (8, 9) and was thus used as a control. Figure 2 shows that both isoforms were expressed at similar levels. The PMCA3CII (3a) protein migrated in the gel faster than PMCA4CI (4b), since its molecular mass is 129 kDa as compared to the 135 kDa of the latter protein. Western blotting analysis using antibody 5F10 (Figure 2B, lane 2), that recognizes all PMCA isoforms (23), and an antibody that only recognizes the N-terminal domain of PMCA3 (Figure 2C, lane 2) (2) showed that the 129 kDa band indeed was PMCA3CII (3a). To characterize the isoform, partial purification was performed on solubilised membranes of expressing cells using a calmodulin sepharose column. The procedure removed most unrelated proteins, but contaminants were still visible in silver stained gels of the EDTA eluates (Figure 3A). The binding of calmodulin to the partially purified PMCA3CII (3a) pump was estimated on nitrocellulose sheets by exposing them to different concentrations of biotinylated-calmodulin. A typical experiment is shown in Figure 3B. The 129 kDa band bound calmodulin at 1 μM and at 10 nM in the presence of Ca^{2+}, but not at 1 nM, nor at 1μM when the membranes were incubated with EGTA. A band of unknown nature migrating at the front of the gel (<20 kDa) bound calmodulin when the latter was present in high concentrations, but the binding persisted, albeit weakly, in the presence of EGTA.

Solubilised membrane fractions from cells overexpressing PMCA3CII (3a) (Figure 4A) formed a strong radioactive band at 129 kDa in acidic gels when incubated with ^{3}-^{32}P-ATP in the presence of Ca^{2+} and La^{3+}. As expected of a PMCA phosphointermediate the band was weaker in the absence of La^{3+}. The band with lower molecular mass evidently corresponded to the endogenous SERCA pump, since its intensity was similar in the presence

and absence of La^{3+}, and since it was sensitive to thapsigargin (not shown). The additional radioactive band in the gels was unlikely to be a degradation product of the PMCA, since it was absent in the Western blots and was still seen in the absence of Ca^{2+}. The nature of this band, which seemed to increase in cells expressing PMCA3CII (3a), is presently unknown. That the band at 129 kDa indeed was the phosphorylated intermediate of PMCA3CII (3a) was confirmed by repeating the experiment on the partially purified pump (Figure 4B). A hydroxylamine-sensitive radioactive 129 kDa band was visible in the presence of Ca^{2+} and La^{3+}, but disappeared almost completely in the presence of EGTA. The intensity of the band was strongly reduced by calmodulin. A similar decrease was also observed for PMCA4CI (4b) (not shown), as could have been expected from previous kinetic experiments (29). However, the extent of the decrease was surprising.

The ATPase activity of the partially purified pump was stimulated about 3-fold by calmodulin in the presence of Ca^{2+} (Figure 5A), with maximal stimulation at about 500 nM calmodulin and half-maximal activation at 5-10 nM. These results are in good agreement with the calmodulin overlay experiments of Figure 3. At 10 nM calmodulin, half-maximal stimulation of the ATPase was obtained with 0.3 µM Ca^{2+} (Figure 5B), full stimulation with 2¼M. The V_{max} of the partially purified pump (700-800 nmoles ATP/mg.min) was lower than that of the full length PMCA4 purified from insect cells (1,100-1,400 nmoles ATP/mg.min). These values only indicative, since the degree of purification of the two pumps may have been different.

Expression and cellular localisation of the expressed PMCA isoforms in CHO cells

To study the roles of PMCAs on the cellular homeostasis of Ca^{2+} the four full-length isoforms and the two truncated variants of PMCA3 and PMCA4 were transiently overexpressed in CHO cells. Prior to monitoring [Ca^{2+}] in the cytosol, in the ER and in the mitochondria, the levels of expression of the pumps and their membrane sorting were analysed by Western blot and immunocytochemistry.

The transfection routinely yielded 15–20% positive cells (however, see below for PMCA1), of which 15-20% yielded a pure plasma membrane targeting pattern, i.e., a clear signal at the cell surface (Figure 6). However, in the remainder of the cell population, either no rim staining was visible, showing that the overexpressed PMCA was retained in the ER (these cells indeed gave a pure ER expression pattern in the fluorescence microscope) or both rim staining and ER expression patterns were visible. Most likely, the PMCA units retained in the ER were inactive (30) and thus did not influence Ca^{2+} homeostasis, but were still detected in the Western blots and could thus affect the quantitative estimate of the effects of the pump. The percentage of cells with unambiguous plasma membrane expression pattern was obtained by counting hundreds of cells for each transfection experiment on each isoform. Since the percentages were similar for all isoforms quantitative comparison appeared permissible. At variance with all the pumps PMCA1, only produced successful transfection in about 12% of the cells. The finding reflects common experience that the PMCA1 is particularly difficult to transfect and express. The difficulty has now been shown to reflect the unique propensity of isoform 1 to undergo proteolysis (Guerini et al; in preparation). Fortunately, the percentage of cells with pure plasma membrane expression pattern, was higher for PMCA1 (28.0 ± 5.1% of the successfully transfected cells). The higher value of plasma membrane delivery thus compensated for the lower transfection efficiency of

PMCA1.

The Western blots of Figure 7, which were probed with antibody 5F10, show the level of overexpression of all pumps. In all cases the antibody recognized a 130-135 Kda protein, as expected of PMCAs. The antibody also reacted with a band in control CHO cells (control), which evidently corresponded to the PMCA1 pump which is likely to be the endogenous pump to CHO cells (31). Since the level of overexpression of the transfected PMCAs over the endogenous pump was estimated to be 150-200%, and since the average transfection efficiency was 15-20%, the total (i.e., plasma membrane and ER retained) PMCAs increase over the endogenous pump in successfully transfected cells was estimated to be 3 to 5 fold (depending on the isoform).

Cytosolic Ca^{2+}

CHO cells were co-transfected with the plasmid of cytosolic aequorin (cytAEQ, 26) and the expression vector coding for the PMCAs isoforms. After aequorin reconstitution (see the Experimental procedures section) cells were incubated in the modified KRB medium supplemented with 1 mM $CaCl_2$ and challenged after about 1 min with the inositol 1,4,5-trisphosphate ($InsP_3$)-generating agonist ATP. The challenge induced a cytosolic $[Ca^{2+}]$ transient, $[Ca^{2+}]_C$, which in control cells (transfected only with cytAEQ) reached a peak value of 3.29 ± 0.32 μM (n=39) and decayed to the baseline within about 3 minutes (Figure 8). The Figure also shows the $[Ca^{2+}]_C$ transients in cells overexpressing the PMCA isoforms. Panel A refers to the full length variants, Panels B and C to cells overexpressing PMCA3CI (3b) and CII (3a), and PMCA4CI (4b) and CII (4a), respectively. The peak values and the time for half decay of the $[Ca^{2+}]_C$ transients are summarised in Table I. Both the amplitude and the duration of the agonist-dependent $[Ca^{2+}]$ increase were significantly affected by the

overexpression of the PMCAs. While the faster clearance of the signal in PMCA overexpressing cells could be reasonably attributed to the increased exporting activity, the decreased height of the Ca^{2+} peak could be due either to the decreased release of Ca^{2+} from the incompletely filled intracellular stores (i.e., the ER) or to the more efficient dissipation of the [Ca^{2+}] transient by the overexpressed PMCAs. The two ubiquitous isoforms, PMCA1 and PMCA4 (traces *a* and *b*), were less effective than the neuronal isoforms, PMCA2 and PMCA3 (trace *d* and *c*).

ER Ca^{2+}

As shown in previous work (30), the overexpression of PMCA isoform 4 reduced the ER Ca^{2+} level by about 15-20 % with respect to control cells. The reduction was explained with the decrease of resting $[Ca^{2+}]_c$. As it proved impossible to demonstrate it by aequorin or fura-2 experiments the influence of the PMCA isoforms on resting cytosolic [Ca^{2+}] was evaluated indirectly by measuring the resting ER concentration, $[Ca^{2+}]_{er}$. CHO cells were transfected with the construct for the low Ca^{2+} affinity ER-targeted aequorin (erAEQ; 27) or co-transfected with those for erAEQ and the PMCA isoforms. All PMCA overexpressing cells (except those overexpressing isoform 1) showed an evident reduction in the ER Ca^{2+} content (Figure 9 and Table II). The effect was more marked in neuronal isoforms PMCA2 and 3 (30-35%), suggesting that these isoforms are not only more efficient in dissipating the agonist generated cytosolic [Ca^{2+}] transients but also in controlling the basal $[Ca^{2+}]_c$ values, and in turn those of the $[Ca^{2+}]_{er}$. In cells expressing PMCA1CI (1b) a possible

minor difference in the ER [Ca^{2+}] could have gone undetected. No obvious differences in the effect on $[Ca^{2+}]_{er}$ were observed between the C-site truncated isoforms of PMCA3 and 4 and the corresponding full-length variants, in agreement with the results obtained with cytAEQ.

Mitochondrial Ca^{2+}

Next, experiments were performed to explore whether the decrease in the level of ER Ca^{2+} filling produced by the expression of the PMCAs affected mitochondrial Ca^{2+}, $[Ca^{2+}]_m$. Cells were transiently transfected with the construct for low Ca^{2+} affinity mitochondrial aequorin (mtAEQ) alone, or co-transfected with those for mtAEQ and for the PMCAs (Figure 10). As expected, ATP induced a large transient increase in $[Ca^{2+}]_m$ in control cells (peak value 57.57 ± 15.65 μM, n=34). The height of the peak was reduced by about 33 and 45% in PMCA1 and PMCA4 overexpressing cells, respectively, but by much more, i.e., by about 70-75%, in PMCA2 and 3 overexpressing cells (panel A and Table III). Isoforms 3CI (3b) and 3CII (3a) (traces *c* and *e*, respectively in panel B) reduced the mitochondrial Ca^{2+} transient by a similarly large extent. By contrast, and surprisingly, isoform 4CII (4a) (panel C, trace *f*) was significantly more efficient than the corresponding full-length isoform 4CI (4b) (panel C, trace *b*). Since the $InsP_3$-modulated channels produce [Ca^{2+}] hotspots that are sensed by neighbouring mitochondria, the peak height of the mitochondrial [Ca^{2+}] transient would be expected to reflect differences in ER Ca^{2+} filling. However, the result with PMCA1CI (1b) was not in line with the expectation. The overexpression of this isoform

reduced by about 35% $[Ca^{2+}]_m$, but produced no clear difference in $[Ca^{2+}]_{er}$. This may have reflected ER heterogeneity not revealed by the ER targeted aequorin, but other factors may have played a role, since the conditions for the monitoring of $[Ca^{2+}]_{er}$ (resting cells) and of $[Ca^{2+}]_m$ (stimulated cells) were different.

Discussion

Considering their peculiar tissue distribution of the PMCA pump isoforms it would be logical to relate it to specific Ca^{2+} homeostasis demands of tissues, and/or of cells in their various developmental/functional stages. This would in turn demand that key properties of the isoforms, i.e., Ca^{2+} affinity, calmodulin sensitivity, sensitivity to other regulatory processes, differ sufficiently to accommodate specific Ca^{2+} homeostasis requests. Unfortunately, the information presently available on functional differences among isoforms is fragmentary at best. The problem is further exacerbated by the existence, next to the four basic gene products of the pump, of numerous alternatively spliced variants, which also display tissue-specific expression and which in some cases may be even more abundantly expressed than the un-spliced versions (12, 13). Although the most extensively studied splice variants involve splice site C in the C-terminal cytosolic unit, splice variants involving site A, located immediately downstream of the domain that mediates the regulatory action of acidic phospholipids in the N-terminal half of the pump would also be however potentially interesting. Overexpression of a variant of PMCA2 spliced at site A failed to reveal significant functional differences with respect to the corresponding un-spliced pump (8). The scarce information on functional differences among isoforms unfortunately originates from work on pumps in the purified state or in isolated membrane preparations, not on pump isoforms within the cell environment. Some of the information available in the literature nevertheless deserves to be quoted. Thus, it has been found that the full-length PMCA2 had particularly high calmodulin affinity (8) (apparent K_m= 2-4 nM), whereas **e**xpressed C-terminal peptides containing spliced-in site C inserts, within the calmodulin-binding domain,

interacted with calmodulin with peculiar pH sensitivity (10). The truncated (CII, a) version of PMCA4 overexpressed in insect cells interacted with calmodulin with an apparent K_m of 600-700 nM, as compared to 30-40 nM for the corresponding full-length variant (9), but had significantly higher Ca^{2+}-ATPase activity in the absence of calmodulin. Truncation of the pump resulting from a spliced-in insertion after the 15^{th} residue of the calmodulin-binding domain produced a pump variant termed PMCA3f (corresponding to PMCA3CVI) which has the shortest C-terminal cytosolic unit so far described for PMCA pumps. This variant**,** which is the major isoform in rat skeletal muscles, was only negligibly stimulated by calmodulin in membrane preparations of overexpressing COS cells, even if it still bound to calmodulin columns (13).

The finding that isoform 3CVI (3f) had lost almost completely calmodulin regulation has been the main motivation for the decision to clone, express, and characterise the 3CII (3a) version of this isoform which is homologous to 4CII (4a), which interacts with calmodulin, with very lower affinity. As all other CII (a) variants, the 3CII (3a) variant becomes truncated at the 1117^{th} residue, within the calmodulin-binding domain (32). PMCA3CII (3a) was thus predicted to retain, at best, the some modest degree of calmodulin regulation of PMCA4CII (4a). It was thus surprising to find that it instead reacted with calmodulin with an affinity which was even higher than that of the full-length PMCA4 (K_m = 5-10 nM) and was in fact in the same range of that of PMCA2, which has the highest calmodulin affinity of all PMCAs. It is thus clear that no generalisation can be made on the effects of C-terminal truncation on the affinity for calmodulin, since the process may lead to a pump with markedly decreased affinity (PMCA4CII, 4a), to one that has all but lost calmodulin regulation (PMCA3CVI, 3f)**,** but also to pump variants that retain optimal calmodulin

affinity, as in the case of the PMCA3CII (3a) variant studied here. The finding that some isoforms may interact with calmodulin with very high affinity, whereas others may have poor to extremely poor affinity for it, is interesting in principle, but cannot be placed in a logical physiological framework in the absence of reliable information on the amount of calmodulin available to the pumps within cells.

The experiments reported here have thus evaluated the activity of the isoforms in the native cellular environment. They lead to some conclusions of general significance. The first is that the two ubiquitous isoforms PMCA1 and PMCA4 are far less effective in controlling the homeostasis of Ca^{2+} than the two neuron-specific isoforms PMCA2 and PMCA3. The second is that the CII (a) truncated versions of the two pumps studied (one ubiquitous, one tissue-specific) are just as effective in controlling cellular Ca^{2+} than the corresponding full-length variants. Even if truncated isoforms differ widely in calmodulin affinity they all function very efficiently in the intracellular ambient. Therefore, in this ambient the availability of calmodulin may be but one of the factors that regulate the activity of the pumps. Other factors/processes could take primacy, perhaps depending on particular demands of cell physiology. Interestingly, one of the first studies of PMCA regulation (33) had calculated that in the membrane environment the pump would be permanently activated to about 50% of maximum by acidic phospholipids. The finding that one of the truncated versions (PMCA4CII, 4a) had significantly higher activity in the absence of calmodulin than the full-length counterpart (9)**,** and the demonstration that two C-terminally truncated pumps variants (3CVI, 3f, and 2CII, 2a) were activated by Ca^{2+} at faster rate than the full-length variants of PMCA 2 and 4 (34) would suggest that the truncated variants may dissipate Ca^{2+} spikes at higher rates. Unfortunately, the results of the aequorin experiments described here,

have made the suggestion invalid, shedding no light on the (physiological) rationale for the existence of the CII (a) versions of the pumps.

The targeting of aequorin to the cytoplasm and to the organelles has shown that the PMCA pumps efficiently regulate the homeostasis of Ca^{2+} in all cell areas. The pumps interfered significantly with the Ca^{2+} cross talk between the ER and the mitochondria, which is essential to Ca^{2+} homeostasis. The fluctuations of the mitochondrial [Ca^{2+}] closely reflected the size of the releasable ER Ca^{2+} pool, and may even be a more precise indicator of the Ca^{2+} handling ability of the ER than the level of Ca^{2+} loading of the reticulum itself: the results with PMCA1CI (1b) showed essentially no changes in ER Ca^{2+}, but still revealed evident changes in mitochondrial Ca^{2+}.

Acknowledgements

We thank Dr. M. Mongillo (Padova, Italy) for helping with Bio-Rad 2100MP confocal system. We are indebted to Dr. E.E. Strehler (Rochester, MN) for the kind donation of the cDNA of rat's PMCA3CI (3b) pump. The work has been made possible by the financial contribution of Telethon-Italy (Grants 963 and GP0193Y01), of the Italian Ministry of University and Scientific Research (PRIN2000, PRIN2001), of the National Research Council of Italy (Target Project on Biotechnology), of the Armenise Harvard Foundation, of the Human Frontiers Science Program Organization and of the National Research Council of Italy (Agency 2000).

References

1. Pedersen, P. L., and Carafoli, E. (1987) *Trends Biochem. Sci.*, **12**, 146-150

2. Stauffer, T., Guerini, D., and Carafoli, E. (1995) *J. Biol. Chem.*, **270**, 12184-12190

3. Falchetto, R., Vorherr, T., Brunner, J., and Carafoli, E. (1991) *J. Biol. Chem.*, **266**, 2930-2936

4. Falchetto, R., Vorherr, T., and Carafoli, E. (1992) *Protein Sci.*, **1**, 1613-1621

5. Stauffer, T., Hilfiker, H., Carafoli, E., and Strehler, E. E. (1993) *J. Biol. Chem.*, **268**, 25993-26003

6. Carafoli, E. (1991) *Physiol. Rev.*, **71,** 129-153

7. Carafoli, E. (1994) *FASEB J.*, **8**, 993-1002. Review.

8. Hilfiker, H., Guerini, D., and Carafoli, E. (1994) *J. Biol. Chem.*, **269**, 26178-26183

9. Seiz-Preianò, B. S., Guerini, D., and Carafoli, E. (1996) *Biochemistry*, **35**, 7946-7953

10. Kessler, F., Falchetto, R., Heim, R., Meili, R., Vorherr, T., Strehler, E. E., and Carafoli, E. (1992) *Biochemistry*, **31**, 11785-11792

11. Greeb, J., and Shull, G. E. (1989) *J. Biol. Chem.*, **264**, 18569-18576

12. Filoteo, A. G., Elwess, N. L., Enyedi, A., Caride, A., Aung, H. H., and Penniston, J. T. (1997) *J. Biol. Chem.*, **272**, 23741-23747

13. Filoteo, A. G., Enyedi, A., Verma, A. K., Elves, N. L., and Penniston, J. T. (2000) *J. Biol. Chem.*, **275**, 4323-4328

14. Rizzuto, R., Pinton, P., Carrington, W., Fay, F. S., Fogart, K. E., Liftshitz, L. M., Tuft, R. A., and Pozzan, T. (1998) *Science*, **280**, 1763-1766

15. Brown, B. J., Hilfiker, H., DeMarco, S. J., Zacharias, D. A., Greenwood, T. M., Guerini, D., and Strehler, E. E. (1996) *Biochim. Biophys. Acta*, **1283,** 10-13

16. Summers, M. D. and Smith, G. E. (1998*) A manual of methods for baculovirus vectors and insect cell culture procedures*. Texas Agricultural Experiment Station Bulltin, 1555, Texas A&M University, College Station, USA

17. Luckow, V. A., Lee, S. C., Barry, G. F., and Olins, P. O. (1993) *J. Virol.*, **67**, 4566-4579

18. Rizzuto, R., Brini, M., Bastianutto, C., Marsault, R., and Pozzan, T. (1995) *Methods Enzymol.*, **260**, 417-428

19. Laemmli, U. K. (1970) *Nature*, **227**, 680-685

20. Sarkadi, B., Enyedi, A., Földes-Papp, Z., and Gardos, G. (1986) *J. Biol. Chem.*, **261,** 9552-9557

21. Towbin, H., Staehlin, T., and Gordon, J. (1979) *Proc. Natl. Acad. Sci.* USA, **76**, 4350-4354

22. Stauffer, T. P., Guerini, D., Celio, M. R., and Carafoli, E. (1997) *Brain Res.*, **748**, 21-29

23. Adamo, H., Caride, A. J. and Penniston, J. T. (1992) *J. Biol. Chem.*, **267,** 14244-14249

24. Lanzetta, P., Alvarez, L., Reinach, P. and Candia, O. (1979) *Anal. Biochem.* **100**, 95-97

25. Fabiato, A., and Fabiato, F. (1979) *J. Physiol. (Paris)*, **75,** 463-505

26. Brini, M., Marsault, R., Bastianutto, C., Alvarez, J., Pozzan, T., and Rizzuto, R. (1995) *J.*

Biol. Chem., **270**, 9896-9903

27. Montero, M., Brini, M., Marsault, R., Alvarez, J., Sitia, R., Pozzan, T., and Rizzuto, R. (1995) *EMBO J.*, **14**, 5467-5475

28. Barrero, M. J., Montero, M., and Alvarez, J. (1997) *J. Biol. Chem.*, **272**, 27694-27699

29. Herscher, C. J., Rega, A. F. and Garrahan, P. J. (1994) *J. Biol. Chem.*, **269**, 10400-10406

30. Brini, M., Bano, D., Manni, S., Rizzuto, R. and Carafoli, E. (2000) *EMBO J.*, **19**, 4926-4935

31. Guerini, D., Schröder, S., Foletti, D., Carafoli E. (1995) *J Biol Chem*, **270**, 14643-14650

32. Strehler, E. E., Strehler-Page, M. A., Vogel, G., and Carafoli, E. (1989) *Proc. Natl. Acad. Sci. USA*, **86**, 6908-6912

33. Niggli, V., Adunyah, E. S. and Carafoli, E. (1981) *J. Biol. Chem.*, **256,** 8588-8592

34. Caride, A. J., Penheiter, A. R., Filoteo, A. G., Bajzer, Z., Enyedi, A., and Penniston, J. T. (2001) *J. Biol. Chem.*, **276**, 39797-39804

Figure legends

Fig. 1. Construction of an expression vector for PMCA3CII (3a). The thick black line represents the coding sequence of the pump, between the start codon (ATG) and the stop codon (TGA). The additional regions present in the expression vector at the 5' and 3' end are given by the thin line. The numbering of the restriction sites is according to (15). The arrow indicates the location of the oligonucleotide primers used for the assembly of the full-length vector. Some of the restriction sites are given. The location of the transmembrane domains (shadowed rectangles), and of two important amino acids (D=Asp and K=Lys) involved in the catalytic activity of the pump are also shown.

Fig. 2. Expression of the PMCA3CII (3a) in insect cells. (A) Coomassie Brilliant Blue staining of 30-36 µg of crude membrane proteins from control Sf9 cells (lane 1) and from cells infected with recombinant vectors for the PMCA3CII (3a) (lane 2) and for the

PMCA4CI (4b) (lane 3).

Western blot of the samples of panel A incubated with monoclonal antibody 5F10 (B), which recognizes a conserved region of all pump isoforms surrounding the catalytic domain, and with a PMCA3 specific antibody, 3N; for details see (5) (C). The calculated molecular mass of PMCA3CII (3a) is 129 kDa.

Fig. 3. Partial purification of the recombinant PMCA3CII (3a) and binding of calmodulin to it. Partial purification of the PMCA3CII (3a) protein expressed in Sf9 cells by affinity chromatography on a calmodulin-sepharose column (A). Silver staining (SS) and Western blot (5F10) (using 5F10 monoclonal antibody, see also figure 2B) of crude membrane proteins before purification (lane 1) and after purification (lane 2).

Calmodulin overlay on about 0.5 µg partially purified PMCA3CII (3a) protein (B). After transfer from the gel to the nitrocellulose, the sheet was incubated in the presence of Ca^{2+} and 1 µM, 10 nM and 1 nM biotinylated calmodulin (lanes 1, 2 and 3) respectively, or in the presence of EGTA and 1 µM biotinylated calmodulin (lane 4). The asterisks indicate the position of PMCA3CII (3a).

Fig. 4. Formation of the phosphoenzyme intermediate by the PMCA3CII (3a). (A) Crude membrane proteins from Sf9 cells infected with recombinant baculoviruses encoding beta-galactosidase (control) and the PMCA3CII **(**3a). Cell membranes were incubated in the presence of $^{3}{}^{32}$P-ATP, and La^{3+} and Ca^{2+} as indicated in the Figure, proteins separated on acidic gels and exposed to autoradiography. The expected positions of the PMCA3CII (3a) and the endogenous SERCA are given by the arrows. Additional details in the Experimental

procedures section.

(B) 1 µg of partially purified PMCA3CII (3a) was phosphorylated in the presence of ^{32}P-ATP, and La^{3+}, Ca^{2+}, EGTA and calmodulin (1 µM) as indicated. The precipitated samples were separated by acidic SDS-PAGE and exposed to autoradiography. The samples in lanes 3 and 4 were from different preparations. The sample in lane 5 was phosphorylated in the presence of Ca^{2+} and La^{3+}, precipitated by TCA and then treated with NH_2OH for 30 min at room temperature prior to separation by acidic SDS-PAGE.

Fig. 5. Ca^{2+} and calmodulin dependent ATPase activity of the partial purified PMCA3CII (3a). The ATPase activity of the purified PMCA3CII (3a) pump was measured in the presence of 3.5 µM free Ca^{2+} and of different concentrations of calmodulin. Each column is the average plus standard deviation of 3-4 measurements from 3 independent purifications (A). ATPase activity of the purified PMCA3CII (3a) measured in the presence of 10 nM calmodulin and different concentrations of free Ca^{2+}. Each point is the average of 2 to 5 independent measurements from 4 independent enzyme preparations (B).

Fig. 6. Immunolocalization of the PMCA1CI (1b) (C), PMCA2CI (2b) (D), PMCA3CI (3b) (E), PMCA3CII (3a) (F), PMCA4CI (4b) (G) and PMCA4CII (4a) (H) in transfected CHO cells. Non-transfected and vector-only transfected control cells are shown in Panels A and B, respectively. The staining with monoclonal antibody 5F10 was revealed by a FITC-conjugated antibody. Immunocytochemistry was performed as described in the Experimental procedures section. Bars, 20µm.

Fig. 7. Western blotting analysis of the isoforms of the PMCA overexpressed in CHO cells. 100 μg of crude membrane proteins from transfected CHO cells, prepared by a freeze and thaw method, were separated by SDS-PAGE as described in the Experimental procedures section and stained with monoclonal antibody 5F10. The control lane corresponds to non-transfected cells. The other lanes correspond to cells transfected with the full-length or truncated variants of PMCAs.

Fig. 8. Monitoring of cytosolic [Ca^{2+}] in CHO cells transfected with cytAEQ and co-transfected with cytAEQ and the full-length or truncated cDNAs of PMCA isoforms. Additional details are described in the Experimental procedures section. Panel A: traces *a*, *b*, *c* and *d* correspond to cells overexpressing isoforms 1CI (1b), 4CI (4b), 3CI (3b) and 2CI (2b), respectively. Panel B: traces *c* and *e* correspond to isoforms 3CI (3b) and 3CII (3a), respectively. Panel C: traces *b* and *f* correspond to cells overexpressing isoforms 4CI (4b) and 4CII (4a), respectively.

Fig. 9. Monitoring of ER [Ca^{2+}] and Ca^{2+} release induced by the $InsP_3$-generating agonist ATP. Additional details on the Ca^{2+} loading and release procedures are found in the Experimental procedures section. Cells were transfected with the low Ca^{2+} affinity erAEQ and co-transfected with the erAEQ and the full-length or truncated variants of PMCA isoforms as indicated. Panel A: traces *a*, *b*, *c* and *d* correspond to cells overexpressing isoforms 1CI (1b), 4CI (4b), 3CI (3b) and 2CI (2b), respectively. Panel B: traces *c* and *e* correspond to isoforms 3CI (3b) and 3CII (3a), respectively. Panel C: traces *b* and *f* correspond to cells overexpressing isoforms 4CI (4b) and 4CII (4a), respectively.

Fig. 10. Monitoring of mitochondrial [Ca^{2+}] in CHO cells transfected with low Ca^{2+} affinity mtAEQ and with mtAEQ and the PMCA isoforms. Additional details are found in the Experimental procedures section. Panel A: traces *a*, *b*, *c* and *d* correspond to cells overexpressing isoforms 1CI (1b), 4CI (4b), 3CI (3b) and 2CI (2b), respectively. Panel B: traces *c* and *e* correspond to isoforms 3CI (3b) and 3CII (3a), respectively. Panel C: traces *b* and *f* correspond to cells overexpressing isoforms 4CI (4b) and 4CII (4a), respectively.

TableI. Cytosolic [Ca^{2+}] in CHO cells transfected with the PMCA isoforms.

	Peak amplitude	Half peak decay time
Control	3.29 ± 0.32 μM; *n* = 39	22.63 ± 7.11 s; *n* = 16
PMCA1CI	2.85 ± 0.42 μM; *n* = 15	13.41 ± 2.50 s; *n* = 7
PMCA2CI	1.40 ± 0.07 μM; *n* = 10	3.19 ± 0.12 s; *n* = 3
PMCA3CI	1.76 ± 0.14 μM; *n* = 7	3.21 ± 0.30 s; *n* = 7
PMCA3CII	1.72 ± 0.30 μM; *n* = 16	4.20 ± 0.62 s; *n* = 9
PMCA4CI	2.40 ± 0.22 μM; *n* = 15	7.90 ± 1.10 s; *n* = 8
PMCA4CII	1.80 ± 0.54 μM; *n* = 16	6.29 ± 2.33 s; *n* = 6

The peak values of the $[Ca^{2+}]_c$ transients and the time for half decay of the $[Ca^{2+}]_c$ produced by the agonist ATP. They are expressed as averaged and the number of experiments. Conditions as in Figure 8.

TableII. Steady-state $[Ca^{2+}]_{er}$ level in CHO overexpressing PMCA isoforms.

	Steady-state
Control	596.26 ± 101.8 μM; *n* = 44
PMCA1CI	597.07 ± 67.85 μM; *n* = 26
PMCA2CI	410.25 ± 97.54 μM; *n* = 10
PMCA3CI	399.55 ± 48.22 μM; *n* = 7
PMCA3CII	407.07 ± 29.42 μM; *n* = 16
PMCA4CI	498.50 ± 64.31 μM; *n* = 15
PMCA4CII	472.55 ± 74.78 μM; *n* = 16

The values are expressed as averaged and the number of experiments. Conditions as in Figure 9.

Table III. Mitochondrial [Ca^{2+}] in CHO cells overexpressing PMCA isoforms.

	Peak amplitude
Control	57.57 ± 15.65 μM; *n* = 34
PMCA1CI	38.33 ± 9.07 μM; *n* = 17
PMCA2CI	16.32 ± 4.84 μM; *n* = 11
PMCA3CI	17.14 ± 0.14 μM; *n* = 8
PMCA3CII	13.63 ± 3.21 μM; *n* = 8
PMCA4CI	31.67 ± 5.66 μM; *n* = 9
PMCA4CII	14.54 ± 4.90 μM; *n* = 13

The peak values of the $[Ca^{2+}]_m$ transients produced by the agonist ATP. They are expressed as averaged and the number of experiments. Conditions as in Figure 10.

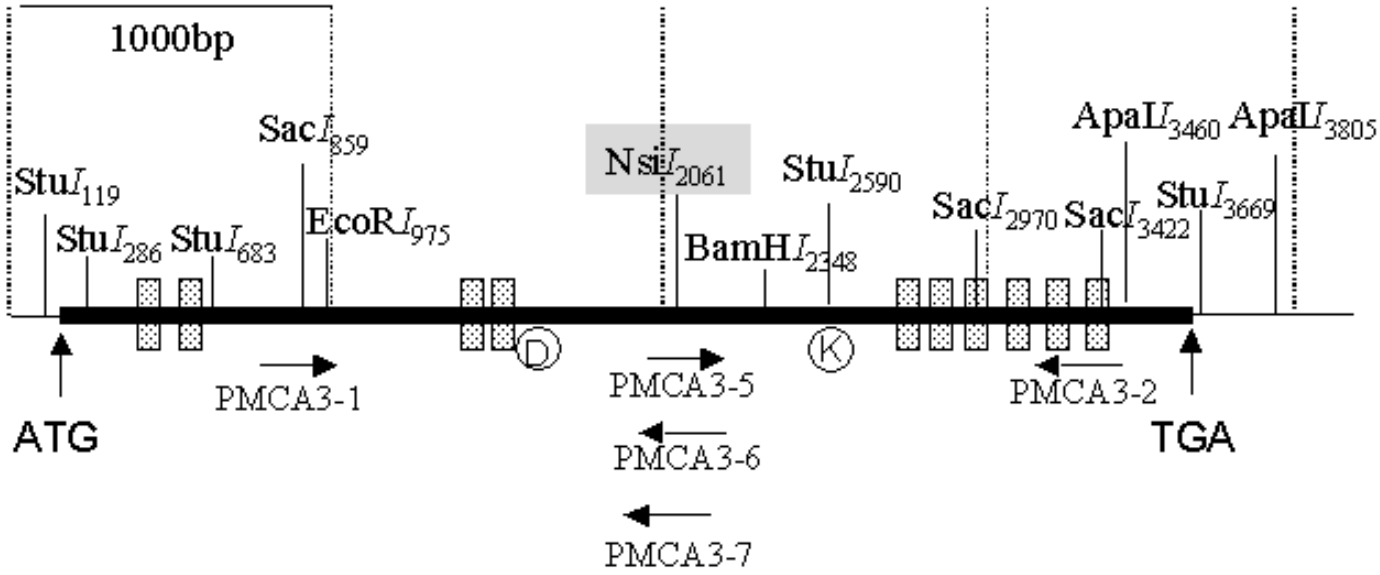

Figure 1

Brini et al.

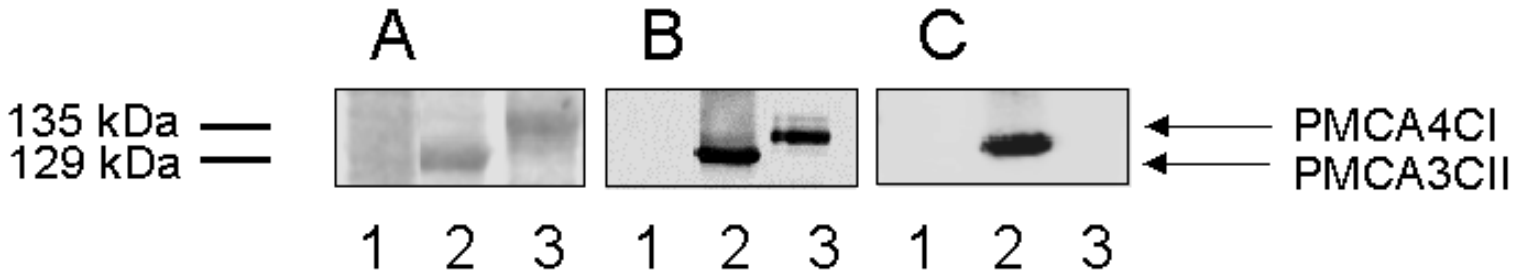

Figure 2
Brini et al.

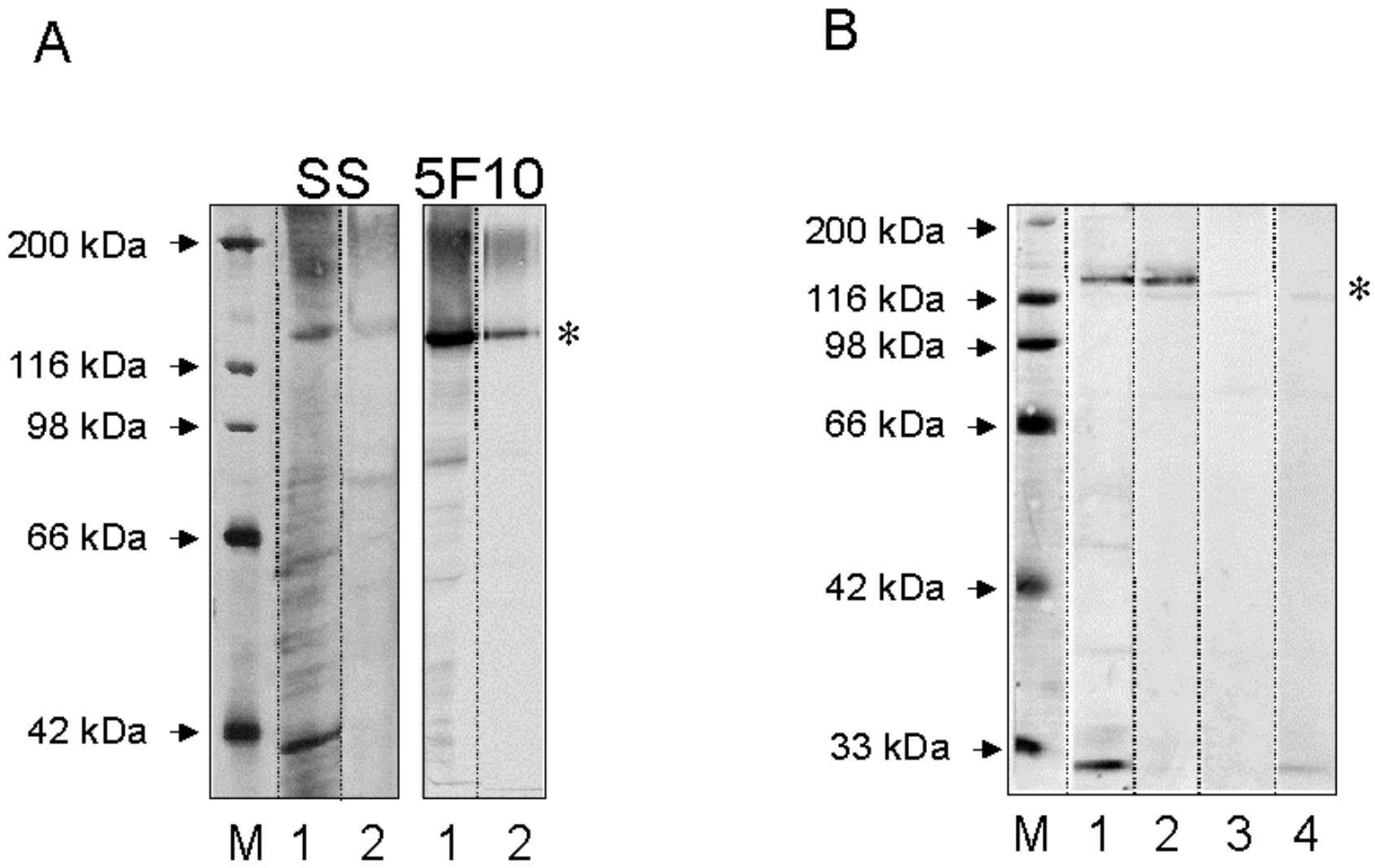

Figure 3
Brini et al.

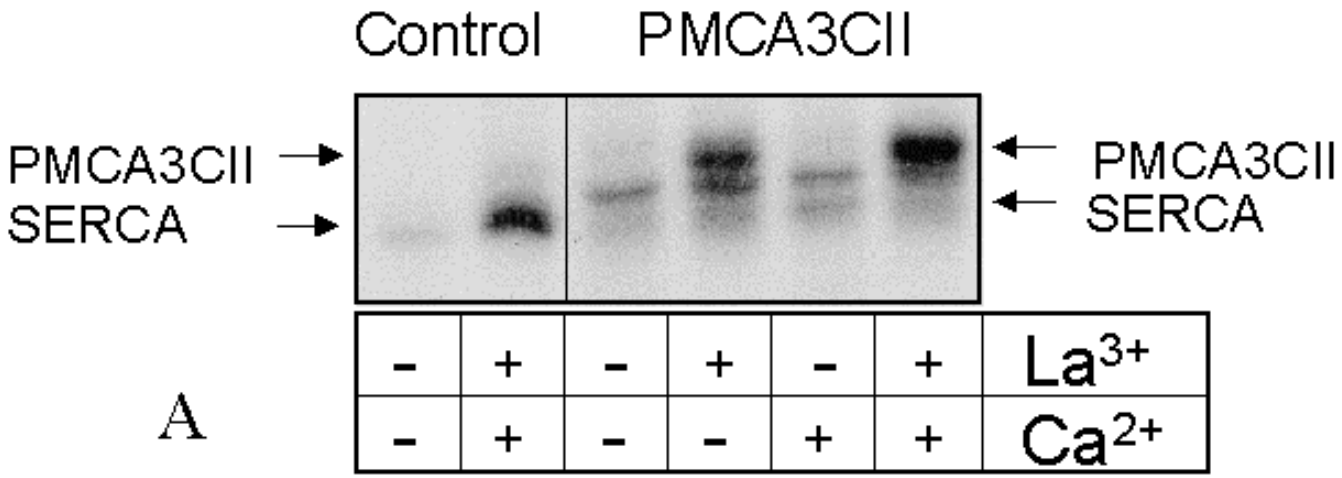

A

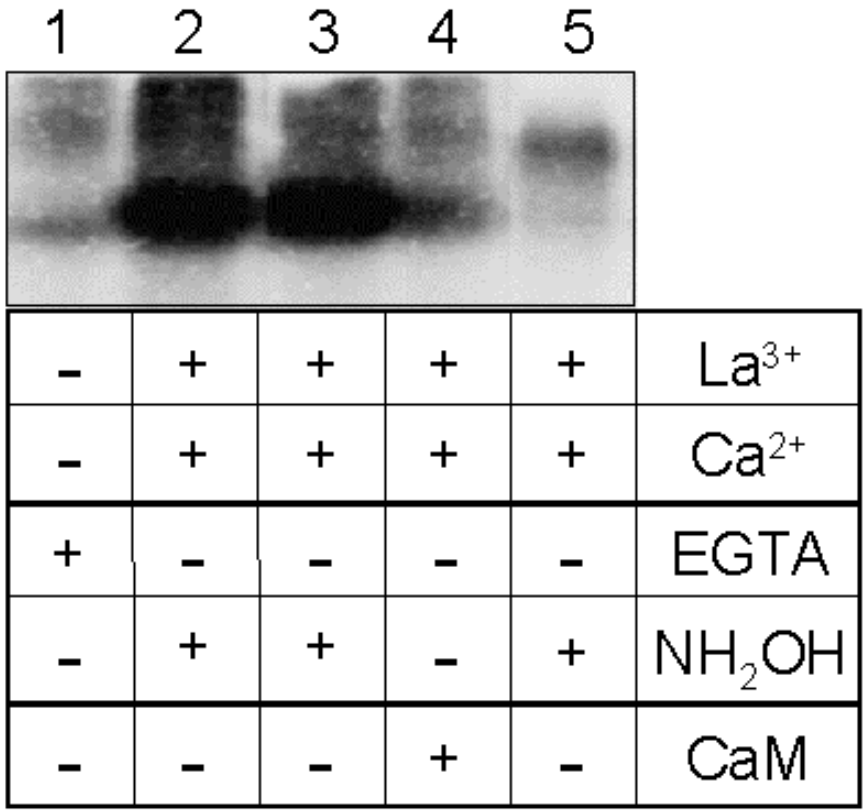

B

Figure 4
Brini et al.

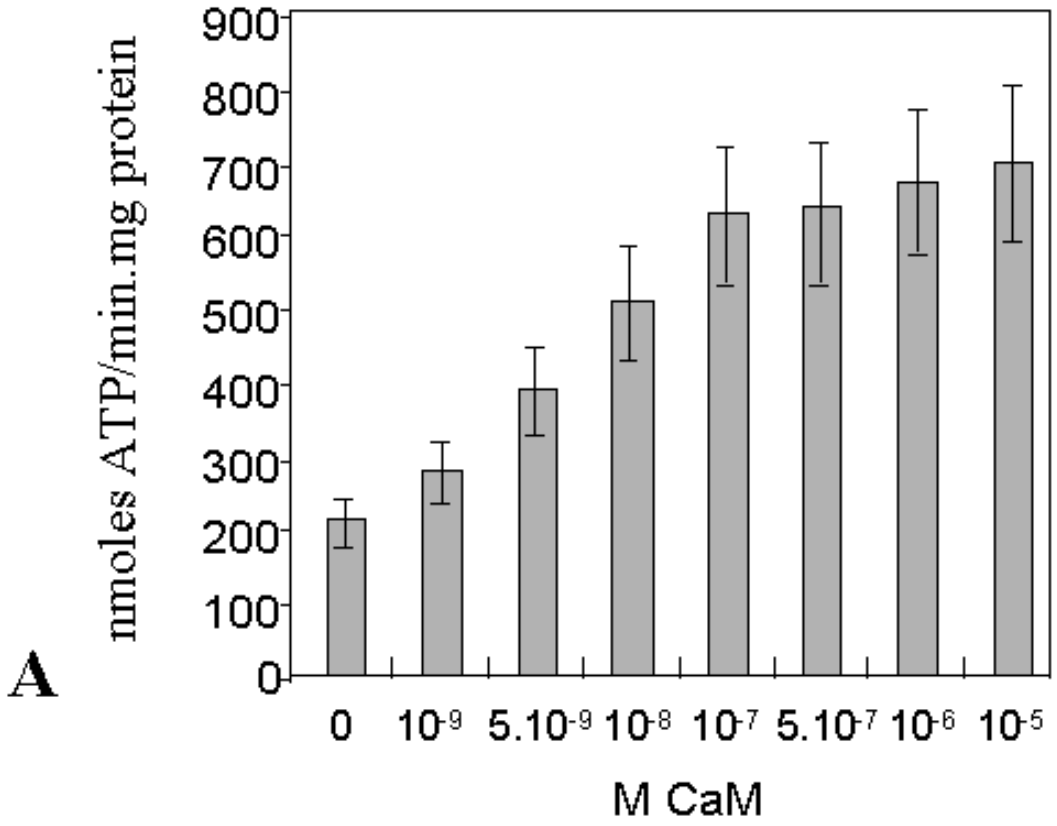

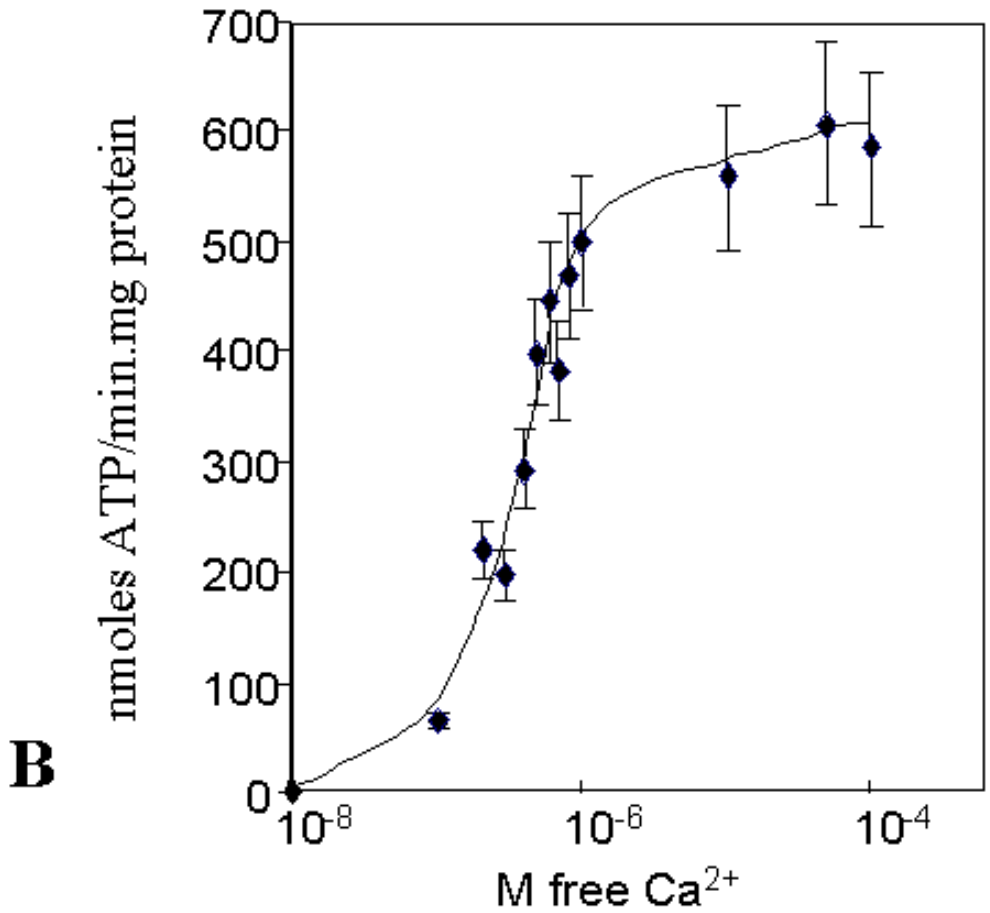

Brini et al.
Figure 5

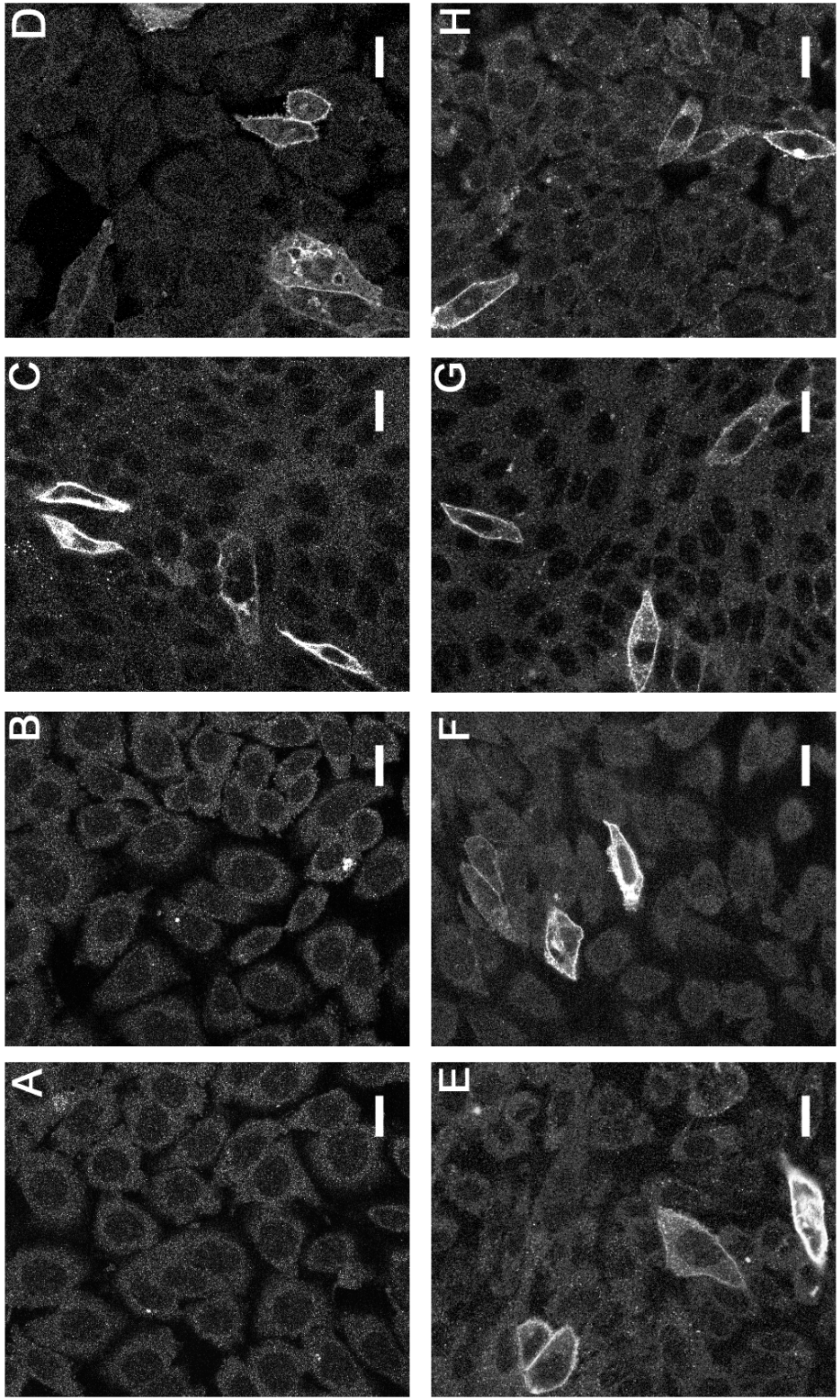

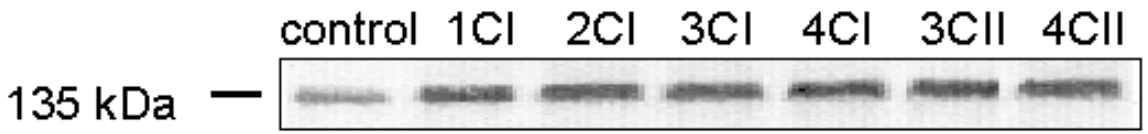

Figure 7
Brini et al.

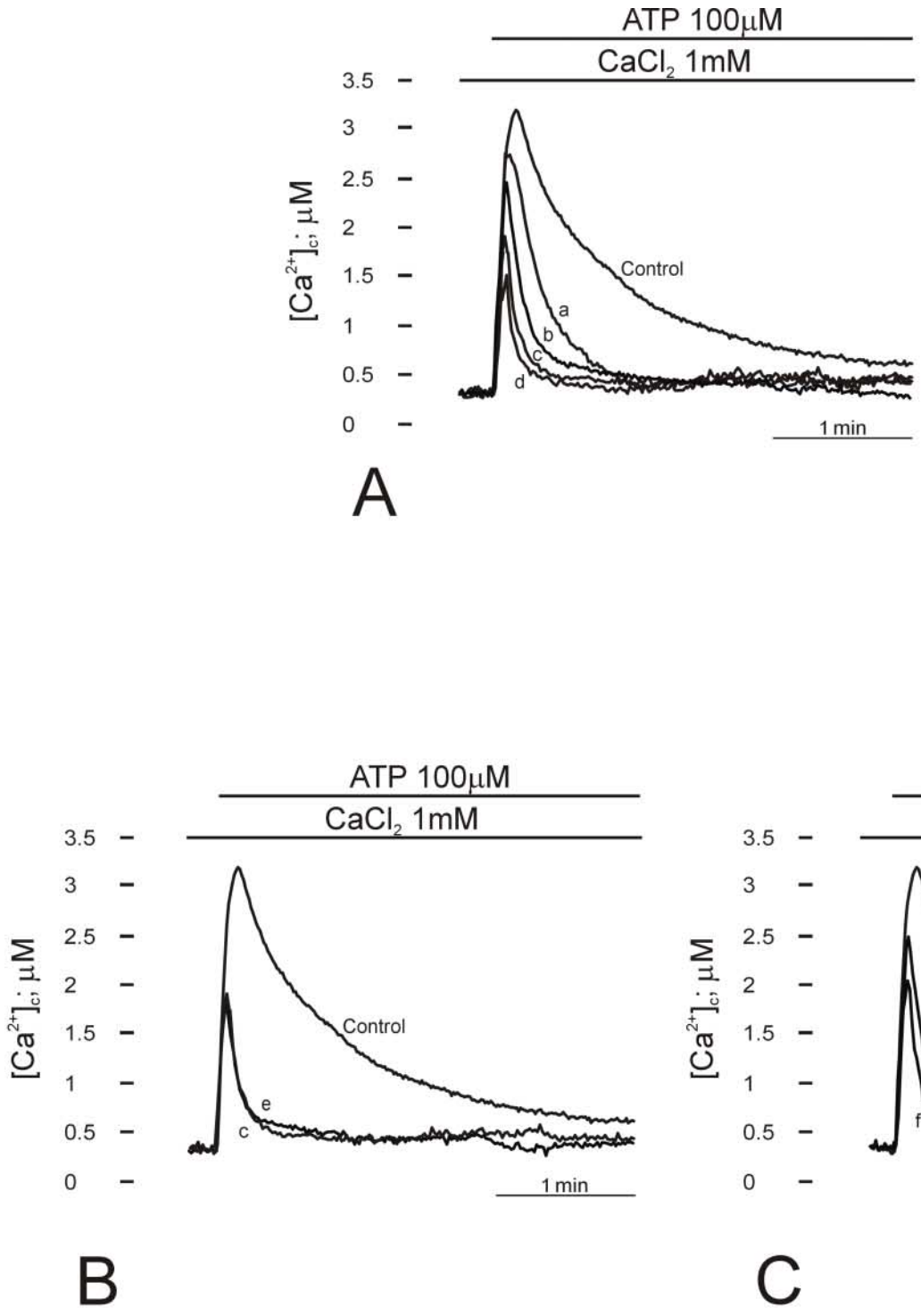

Figure 8
Brini et al.

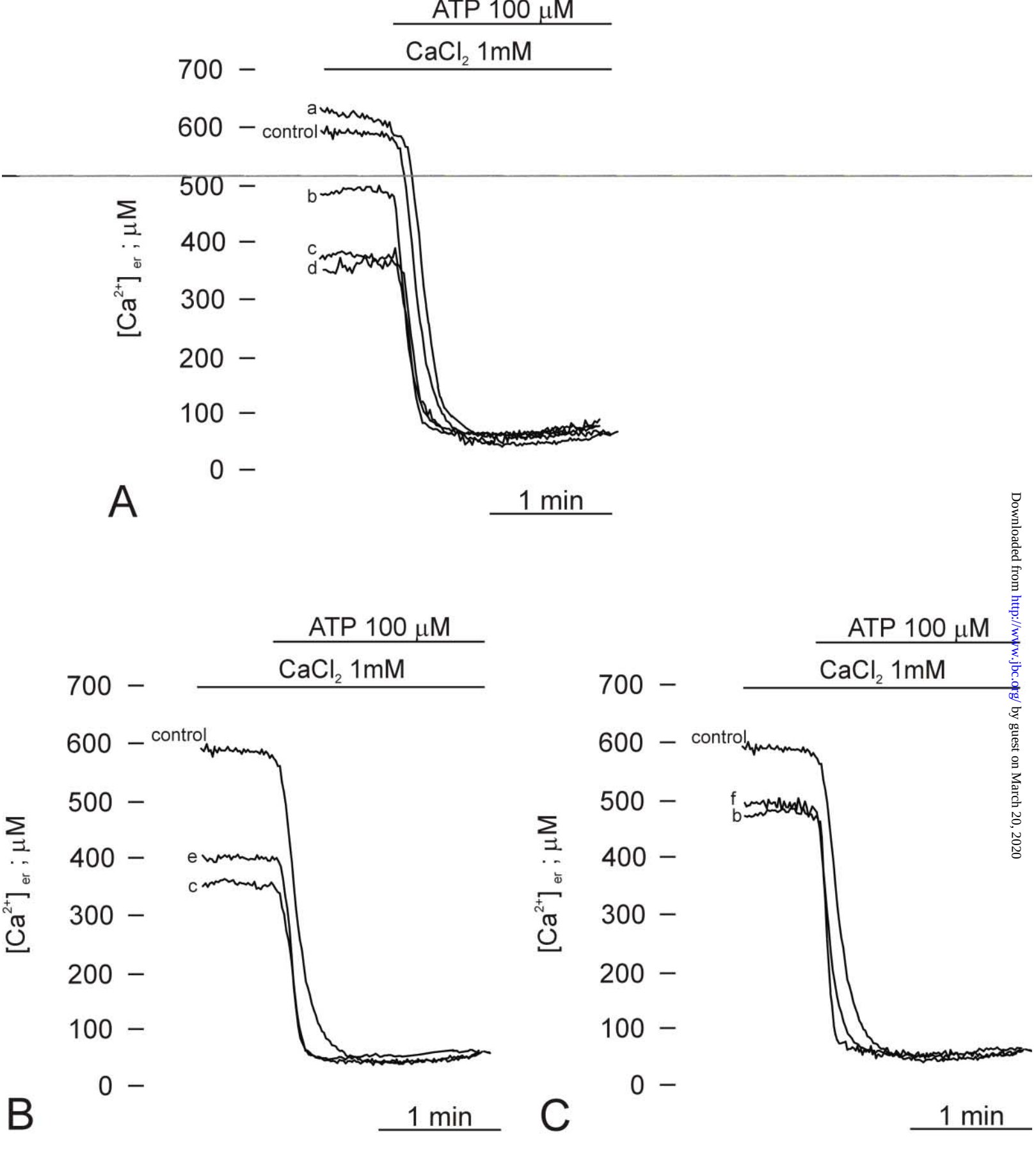

Figure 9

Brini et al.

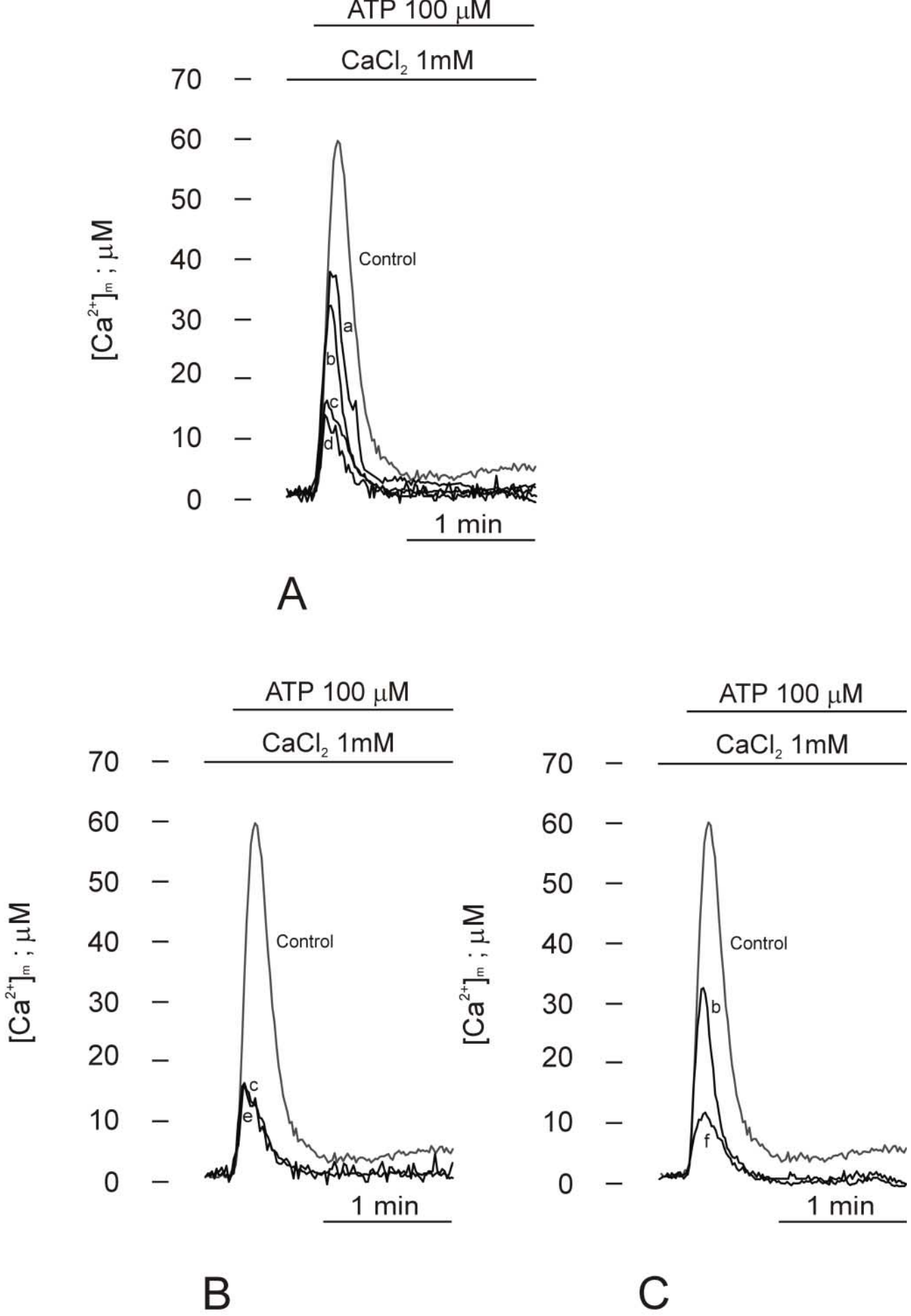

Figure 10
Brini et al.

A comparative functional analysis of plasma membrane Ca2+ pump isoforms in intact cells

Marisa Brini, Luisa Coletto, Nicola Pierobon, Natasha Kraev, Danilo Guerini and Ernesto Carafoli

J. Biol. Chem. published online April 25, 2003
